Serican Journal of Medicine
2025, VOL. 2, NO. 1, 23169
https://doi.org/10.17161/sjm.v2i1.23169

Oxidative stress-associated gene signature predicts the prognosis and therapy response in prostate adenocarcinoma

Bohan Xu[1,2,*], Shen Lin[1,2], Kai Yang[1,2,*]

[1]Department of Urology, The First Affiliated Hospital, Zhejiang University School of Medicine, Hangzhou 310003, China; [2]Zhejiang University Cancer Center, Hangzhou 310058, China; ***Corresponding author** Bohan Xu: bohanxu@zju.edu.cn, ORCID: 0009-0007-7054-5021; Kai Yang: kaiyang@zju.edu.cn, ORCID: 0000-0003-1542-6437

ABSTRACT

Background: Oxidative stress contributes to the development of prostate adenocarcinoma (PRAD). However, the prognosis prediction and therapy response predicted based on oxidative stress-associated genes lacked comprehensive study. Herein, an integrated bioinformatics approach was adopted to identify the prognosis-associated oxidative stress genes for prostate cancer.

Methods: From Gene-Expression Omnibus (GEO) and The Cancer Genome Atlas (TCGA) databases, the transcriptomic data and clinical data were collected. Genes related to oxidative stress were retrieved from oxidative stress pathway "GOBP_RESPONSE_TO_OXIDATIVE_STRESS" in the MsigDB. A risk model was constructed based on the hub genes selected by both WGCNA and LASSO analysis. RT-qPCR analysis and CCK-8 were carried out to validate the results. GEO cohort was used for verifying the model robustness. By running CIBERSORT and ESTIMATE algorithm, immune cell infiltration was quantified. TIDE algorithm and Spearman correlation analysis were used for evaluating the immunotherapy response and drug sensitivity.

Results: We established oxidative stress-related gene signature (NUDT7, NTRK3, MAP3K12, DRD5, C3orf18, and B3GALT2) as an independent factor for the prognostic survival of prostate cancer. *In virto* experiments showed that MAP3K12 had a higher expression in prostate cancer cell lines, and knockdown of MAP3K12 inhibited PC3 cell viability. The risk score was positively linked with T_cells_regulatory_Tregs and Macrophages_M2 and negatively linked with Plasma_cells. High-risk patients showed higher expressions of PDCD1, CD274, CTLA4, LAG3, PDCDILG2, BTLA, HAVCR2, TIGIT, and higher myeloid-derived suppressor (MDSC) score. Docetaxel, Cisplatin, and Bicalutamide could benefit low-risk patients more. Calibration curves and DCA showed an accurate prediction by the nomogram.

Conclusion: We established a novel and reliable prognostic model for prostate cancer patients.

ARTICLE HISTORY
Received: Dec. 4, 2024
Revised: Dec. 26, 2024
Accepted: Jan. 6, 2025

KEYWORDS
prostate adenocarcinoma, oxidative stress, risk model, prognosis, therapy response, chemotherapy sensitivity

EDITED BY
Jindan Yu

REVIEWED BY
Siyuan Cheng, Changshen Zhao

Introduction

Prostate cancer is a heterogeneous cancer [1] that ranks the most frequently diagnosed male cancer in most countries [2, 3]. The latest statistical showed that prostate cancer (PCa) is the fourth most frequent malignancy and the eighth major cancer-correlated death cause, with more than 1,466,680 new cases and 396,792 deaths in 2022 [4-6]. Prostate adenocarcinoma (PRAD) as the most common subtype of PCa is usually diagnosed at an advanced stage. However, treatment of prostate cancer is difficult because we lack clear early clinical symptoms of prostate cancer, which often results in a late diagnosis and excludes the chance for taking surgery on one hand, at the same time, the use of prostate-specific antigen is the most frequently applied indicator for the diagnosis and prognosis of prostate cancer but its application was limited by its poor specificity [7]. Other therapeutic strategies, such as radiotherapy, chemotherapy, androgenic suppression, or immunotherapy may provide survival benefit for patients with advanced prostate cancer [8-10], but personalized therapy remained a major challenge. Hence, it is helpful to identify multiple biomarkers to more accurately predict the prognosis for patients with prostate cancer.

The occurrence and development of cancer are closely related to oxidative stress. The initiation and developed of human cancers involves the critical role

of oxidative stress [11-14], which refers to the imbalance of the generation of reactive oxygen species (ROS) that disrupts endogenous antioxidant defense mechanisms against reactive intermediates and affects the repair of damages to the organs and cellular systems [15]. Increased ROS can lead to proteins, DNA, membrane lipids damage, and dysfunctions to signal transduction pathways, normal cellular function, and cell death [16]. Oxidative stress also contributes to the prostate cancer development [17]. Specifically, prostate cancer is predominant among older men and age-associated functional loss is related to the accumulation of oxidative damages resulted from ROS [18]. In addition, previous studies have shown that oxidative stress-targeted therapy can effectively inhibit the survival of cancer cells [19]. In comparison, research on global genes faces numerous difficulties. Key information is easily obscured by the vast number of genes, making it hard to identify effective targets. Therefore, focusing on oxidative stress-related genes is helpful for the prognostic prediction of prostate cancer and promotes personalized treatment.

Against the backdrop of in-depth exploration of the diagnosis and treatment dilemmas of prostate cancer, clarifying the close connection between oxidative stress and the occurrence and development of cancer has pointed out the direction for research. Studies found that multiple prognostic genes identified by recent bioinformatics analyses were integrated into a single prognosis model, which can predict the prognosis and improve treatment response [20]. Thus, this study was designed to screen prognostic genes based on oxidative stress for prostate cancer patients and establish a prognostic model to further improve prediction accuracy. To determine the hub genes from TCGA-PRAD cohort, WGCNA and LASSO Cox regression analysis were employed. A risk model was developed based on risk score and its robustness was verified in a GEO cohort. The two risk types were analyzed in terms of gene mutation characteristics, pathway characteristics, immune microenvironment, and immunotherapy response. Finally, we probed into the connection between the risk score and drug sensitivity.

Material and methods

Data collection and processing

The RNA-sequencing analysis was performed according to the clinical data and gene expression profiles of prostate cancer patients downloaded from the TCGA-PRAD (https://portal.gdc.cancer.gov/) project using Genomic Data Commons Application Programming Interface. A total of 459 primary prostate cancer samples were obtained. Among these, patients without clinical status or follow-up data were deleted, keeping those with survival time longer than 30 days. Gene symbol IDs were converted from ensembl gene IDs. The gene expression profiles of GSE70769 [21] containing 92 prostate cancer samples was obtained from GEO (https://www.ncbi.nlm.nih.gov/geo/) database and used as a validation cohort. Further, based on the annotation information, probes were mapped to the gene and those matched to multiple genes were excluded. The median value of a gene matching to multiple probes was taken. The "limma" package [22] in R software was employed to process and normalize the raw data from the above data.

Oxidative stress-related genes were collected from "GOBP_RESPONSE_TO_ OXIDATIVE_STRESS" in the Molecular Signatures Database (MsigDB, https://www.gsea-msigdb.org/gsea/msigdb).

Development of a risk model and verification

For identification of oxidative stress related modules, "WGCNA" package [23] in R was employed to conduct WGCNA analysis. The soft-thresholding powers $\beta = 7$ was selected. Thereafter, average-linkage hierarchical clustering was performed to transform adjacency matrix into a topological overlap matrix. Cluster analysis was performed using, with each module containing a minimum number of 30 genes. Then, the eigengenes were calculated, and close modules with deepSplit = 2, height = 0.25, and minModuleSize = 30 were merged into a new one. The WGCNA package was employed to setect the modules with high correlation coefficients for the connection between modules and oxidative stress score. Subsequently, the hub gene in the "oxidative stress-associated module" with $|\text{cor}| > 0.4$ and $p < 0.05$ were identified, and genes with the greatest prognostic significance were considered as candidates related to oxidative stress. Furthermore, the range of genes was reduced by LASSO regression analysis using "glmnet" package [24] in R to identify the most crucial prognostic genes.

The formula of the risk score was:

$$\text{Risk score} = \sum \beta i * \text{ExPi},$$

where "β" and "i" refer to the Cox regression coefficient value and the value of gene expression, respectively. According to the threshold value "0", TCGA-PRAD patients were stratified into low- and

high-risk score subgroups. KM analysis and log-rank test were applied to plot survival curve and to assess difference significance, respectively. The validation set was similarly analyzed as the TCGA-PRAD cohort to validate the robustness of the risk model. The packages "timeROC" [25] was also employed to analyze the prediction accuracy.

Cell culture and transfection

RWPE-1 and 3 prostate cancer cell lines (PC3, DU145, C4-2B) as well as nonneoplastic and immortalized adult human prostatic epithelial cells were purchased from ATCC (USA). Those cells were cultured in 5% CO_2 at 37°C. The cells were transfected with small intern RNA (siRNA) synthesized by GenePharma (Suzhou, China) applying Lipofectamine 2000 (Invitrogen, USA).

Quantitative real-time (qRT-PCR) analysis

Total RNA was isolated with RNAiso plus (Takara, Japan). PrimeScript RT reagent Kit (Takara, Japan) was employed to performed reverse transcription, and quantitative PCR (q-PCR) was carried out with SYBR Premix Ex Taq (Takara, Japan) on a thermal cycler (CFX96, Bio-rad, USA). The relative expression of mRNA was determined using β-actin as the loading control by $2^{-\Delta\Delta Ct}$ method. See Table 1 for the primers used.

Table 1. primers of genes

Genes	Forward	Reverse
MAP3K12	GTACTCTCCACACCCCAGGA	GGCTCTCTCCAGCTTCCTTT
b-actin	ACCCAGAAGACTGTGGATGG	CACATTGGGGGTAGGAACAC

Cell viability assay

The transfected cells were planted into a 96-well plate. After cell incubation for 24 hours (h), 10 μL of CCK-8 solution (DOJINDO, Kumamoto, Japan) was added to further incubate the cells at 37 °C for 3 h. Finally, the absorbance in the 96-well plates was measured at 450 nm.

The relationship between clinical characteristics, risk score, and oxidative stress score classification in prostate cancer

Each sample in the TCGA-PRAD cohort was calculatedd with an oxidative stress score using the ssGSEA in "GSVA" package [26] in R. The clinical significance of oxidative stress score in prostate cancer patients was assessed compared according to the associations of clinicopathological characteristics (T Stage, N stage, age and Gleason score), patients' survival and oxidative stress score. T Stage is commonly used to describe the local situation of the primary tumor. T0 indicates no evidence of a primary tumor. T1 to T4 represent progressively increasing tumor sizes. N Stage is used to describe whether the cancer has spread to nearby lymph nodes. N0 indicates no lymph node involvement. N1 indicates regional lymph node metastasis. The overall survival (OS) was evaluated using the "Survminer 0.4.9" packages [27] in R to perform the Kaplan-Meier (KM) analysis.

Enrichment analysis

The "fgsea" package [28] in R was used to identify biological processes pathways involved. Here, all the candidate gene sets in KEGG database were used for GSEA between the two risk groups. The "clusterProfiler" package [29] in R was employed for function annotation. The correlation heatmap between pathway enrichment score and risk score was generated by "ggcorrplot" package [30].

Gene mutation features between the two risk score groups

To assess genomic changes between the two risk score groups in the TCGA-PRAD cohort, the molecular features of TCGA-PRAD were collected from a previous pan cancer study [31]. The correlation among the risk score in the TCGA-PRAD cohort and genomic changes were also analyzed by Spearman correlation analysis using "cor.test" method in R. Difference in somatic mutation between the two groups was compared employing Chi square test.

Assessment of immune cell infiltration

The relative abundance of 22 types of immune cells in prostate cancer was measured by the CIBERSORT algorithm (https://cibersort.stanford.edu/) [32]. Meanwhile, immune infiltration was computed applying the ESTIMATE algorithm [33]. A total of 29 gene signatures associated with immune infiltration were extracted from a past study [34]. The scores of 29 gene signatures were computed for each patient by performing ssGSEA analysis in "GSVA" package [26]. The oncogenic activities of cell-specific signaling pathways such as p53, MAPK, EGFR, VEGF, and PI3K was calculated using The "PROGENy" algorithm [35].

Immunotherapy response prediction

Based on gene expression profiling, immune checkpoint blockade (ICB) could be evaluated by

Fig. 1. Performance of oxidative stress score in TCGA-PRAD cohort. **A** oxidative stress response in TCGA samples. **B** The association between clinicopathological features (Gleason score, T Stage, N Stage, and age) and oxidative stress score. **C** Overall survival differences between low-risk and high-risk groups. **D** Differences of oxidative stress score between clinicopathological characteristics (T Stage, N Stage, Gleason score and age). P < 0.05 was considered statistically significant.

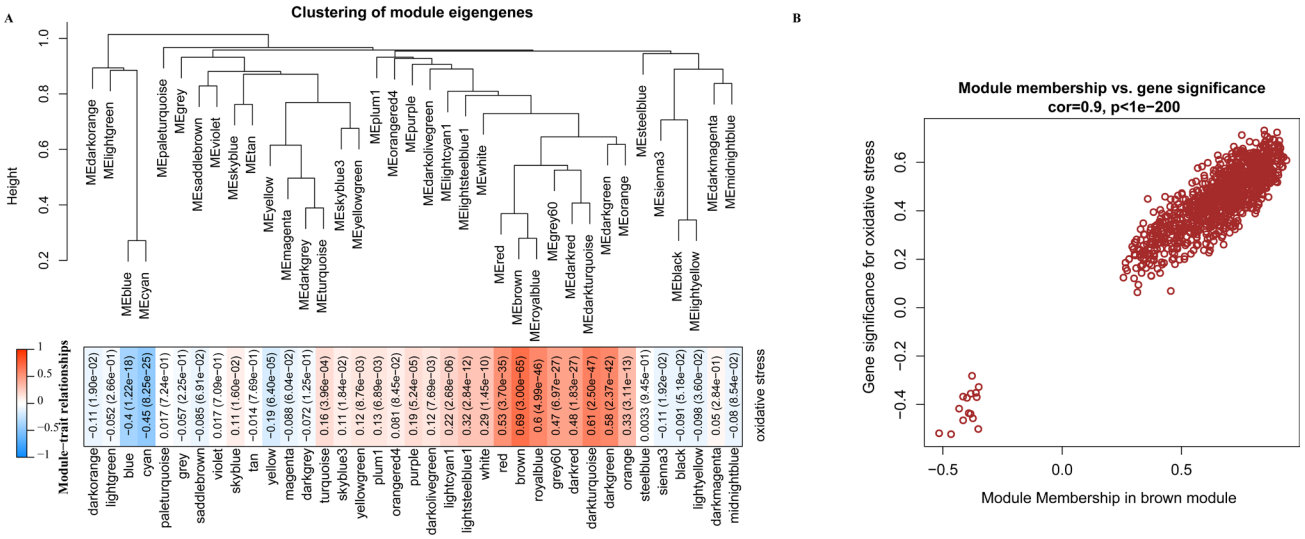

running TIDE algorithm (http://tide.dfci.harvard.edu/) [36]. Clinical responsiveness of patients to ICI therapy was estimated by running TIDE algorithm.

Correlation analysis between the drug sensitivity and risk score

The sensitivity of prostate cancer patients to chemotherapy drugs was analyzed based on GDSC (https://www.cancerrxgene.org/). The connection between drug sensitivity and risk score with |Rs| > 0.2 was subjected to the Spearman correlation analysis, with adjusted FDR < 0.05 as a significant correlation. Then, the "pRRophetic" package [37] in R was employed to calculate IC50.

Development of a nomogram

Independent predictors for the prognosis of prostate cancer cells were selected by performing univariate and multivariate Cox regression analysis. Using "RMS" package [38] in R. The risk score and clinicopathological features were combined to build a nomogram. Calibration plots and DCA were used to assess the reliability of the model.

Statistical analysis

The R version 4.1.2 was employed in all the statistical analyses. The Wilcoxon rank-sum test or Kruskal–Wallis test was used to analyze continuous variables. The Chi-square test was used to analyze the categorical variables, specifically to compare the difference in somatic mutation between the two groups. Spearman correlation analysis was applied to analyze the correlation between the risk score in the TCGA-PRAD cohort and genomic changes as well as to evaluate the immunotherapy response and drug sensitivity. And $p < 0.05$ was considering as a statistical significance.

Results

WGCNA identifies key gene modules related to oxidative stress

Cluster analysis was performed to screen coexpression modules. The soft-threshold power β = 7 was applied to ensure a scale-free network (**Fig S1A-B**). WGCNA sectioned 37 modules (**Fig S1C**), and the grey module could not be merged with other modules. Gene number in each module was presented in **Fig S1D**. Correlation analysis between the oxidative stress score and of the modules showed a significantly positive association between the brown module and oxidative stress (r = 0.69, p < 1e-5) (**Fig 1A**). Moreover, the brown module showed highly positively correlated with module membership (MM) and gene significance (GS) (r = 0.9, p < 1e-5) (**Fig 1B**). Therefore, the brown module was selected as an important gene module related to oxidative stress for further analysis.

Development of risk model and validation

Under the threshold value of |Cor| > 0.4 and p < 0.05, COX regression analysis determined 78 genes

Fig. 2. Oxidative stress related modules identification. **A** Cluster analysis of oxidative stress related genes. **B-C** Network topology analysis with different soft-thresholding powers. **D** Gene cluster dendrogram and the color of modules. E, Number of genes in every module. **F** Correlation analysis between module eigengenes and oxidative stress score. **G** Scatter diagram in the brown module for gene significance vs. module membership. Statistically significant was defined when p < 0.05.

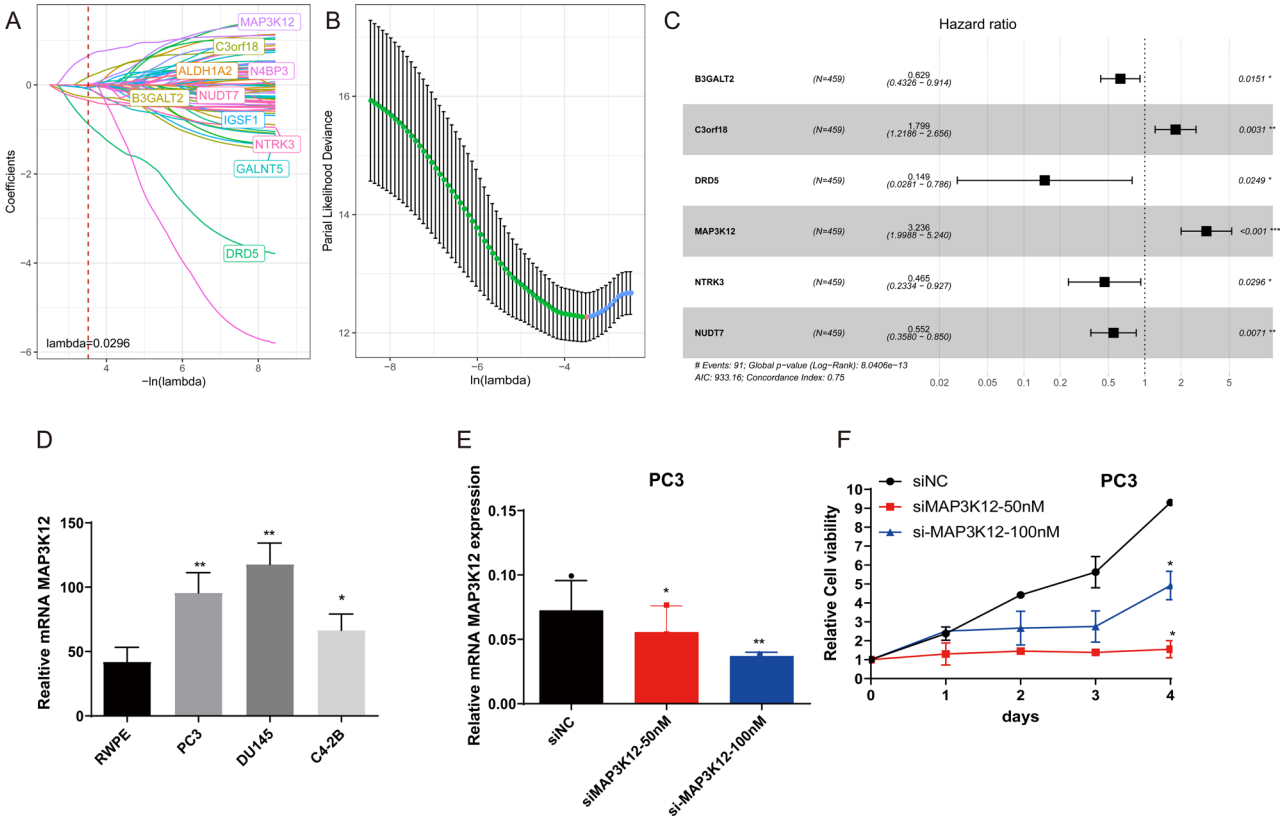

(6 risk and 72 protective genes) that significantly affected the prognosis of prostate cancer ($p < 0.05$) from a total of 680 hub genes in the brown module (**Supplementary Table 1**). LASSO Cox regression analysis showed a steady increase of lambda with increased number of independent variable coefficients close to zero (**Fig 2A**). 10-fold cross-validation was performed and **Figure 2B** displayed the confidence interval under each lambda. We determined 10 genes as the target genes for further analysis when lambda=0.0296. Finally, 6 prognostic genes were defined as the prognostic genes for prostate cancer applying StepAIC (**Fig 2C**).

The risk score formula was: risk score=-0.464*B3GALT2+0.587*C3orf18-1.906*DRD5+1.174*MAP3K12-0.766*NTRK3-0.595*NUDT7.

Our signature identified 6 prognostic genes, among which MAP3K12 was the only variable that showed statistical significance in the multivariate COX regression analysis (Figure 4C). As MAP3K12 showed the most prominent Hazard Ratios, RT-qPCR was performed to measure mRNA level of MAP3K12 in prostate cancer cell lines and a non-tumor human prostate epithelial cell line (RWPE-1). It was observed that the mRNA level of MAP3K12 in prostate cancer cell lines was higher than that in RWPE-1 (**Fig 2D**). Then, we successfully knocked down MAP3K12 using siRNA in prostate cancer (PCa) cells (Fig. **2E**). Moreover, knockdown of MAP3K12 reduced PCa cell viability (**Fig. 2F**). Those data indicated that MAP3K12 may be involved in prostate cancer progression while it also acted as a cancer-promoting gene in the prognostic risk model.

Next, zero-mean normalization was conducted for risk score. It was observed that patients with higher risk scores had more unfavorable prognostic outcomes (**Fig 3A**). The ROC curve (AUC) values of the prognostic model were 0.81, 0.77, and 0.71 for 1 year, 3 years and 5 years, respectively (**Fig 3B**). Low-risk patients showed a greater survival chance than high-risk patients ($p < 0.0001$) (**Fig 3C**). The AUC value of the prognostic model was 0.70 and 0.80 for 5 years and 7 years, respectively (**Fig 3D**) in the validation cohort, and the survival of patients with higher risk was more unfavorable than those with a low risk ($p = 0.017$) (**Fig 3E**).

Fig. 3. Function enrichment analysis on the brown module. **A** The results of KEGG pathway enrichment analysis on the brown module. **B-D** GO functional enrichment results.

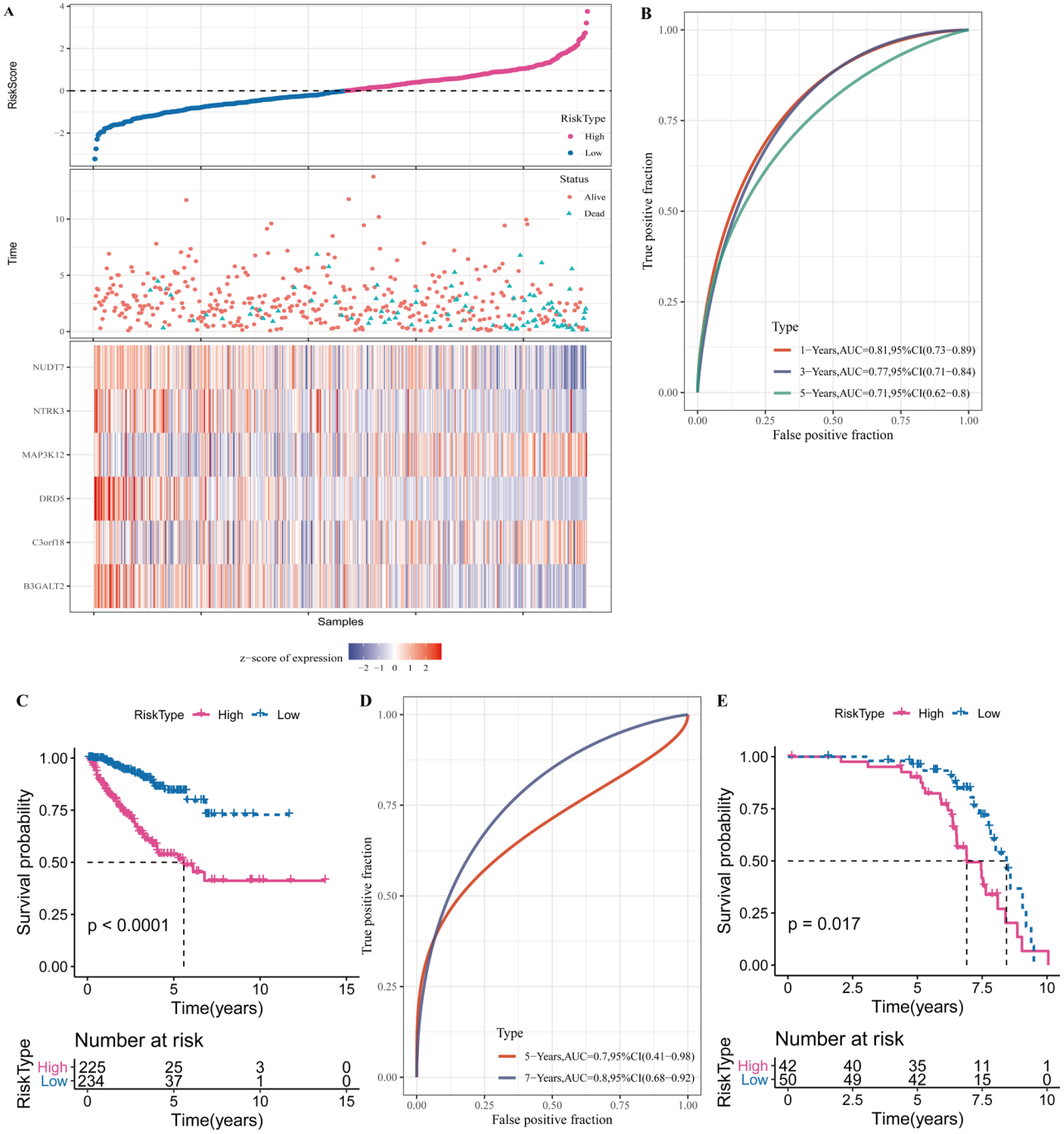

Fig. 4. Risk model development and verification. **A** Independent variable coefficients changed with the increase of lambda. **B** Confidence interval under each lambda. **C** Forest plot of hub genes related to oxidative stress. **D** Distributions of the gene expression, survival status and the risk score. **E** ROC curve and AUC of the prognostic model in evaluating survival for 1 year, 3 and 5 years, **F** Kaplan-Meier curve for the two risk groups of patients in TCGA-PRAD cohort. **G-H** Survival analysis in GEO cohort. Statistically significant was defined when p < 0.05.

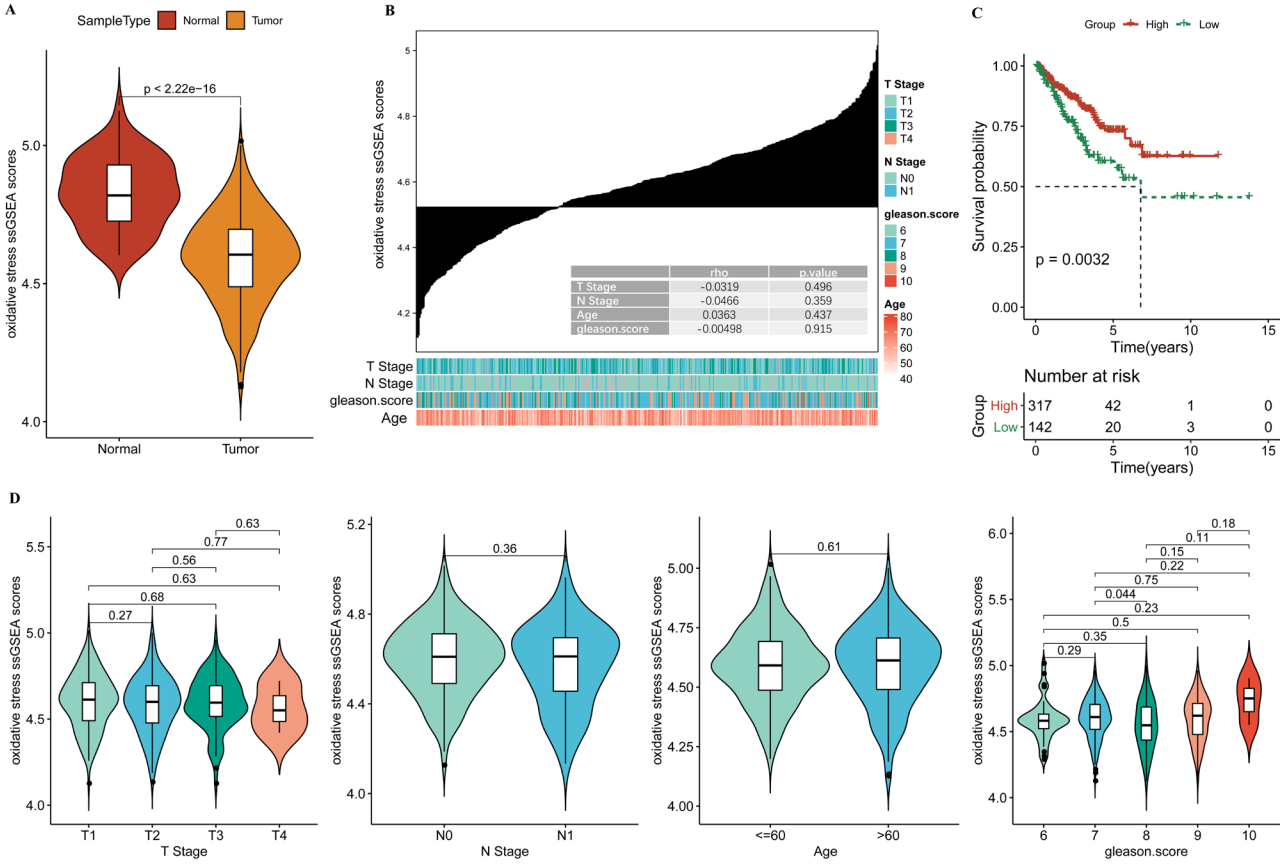

The relationship between prostate cancer and oxidative stress scores

An analysis was conducted on the differences in the oxidative stress responses between prostate cancer samples and adjacent normal tissue samples in the TCGA-PRAD cohort. The results showed that the response of prostate cancer samples to oxidative stress was significantly lower than that of the adjacent normal tissues (**Fig 4A**, $P < 2.22e\text{-}16$). The correlation analysis revealed no significant correlation between clinicopathological characteristics (age, T Stage and N Stage, gleason score) and oxidative stress score (**Fig 4B**). The tumor samples in TCGA-PRAD were classified into high- and low- oxidative stress score groups, with the low-score group having a worse survival than those with a high oxidative stress score (**Fig 4C**). There were also no significant differences in ssGSEA scores between different clinicopathological characteristics (T stage, N stage, gleason score, and age) (**Fig 4D**).

Patients with more advanced clinical grades (gleason score, T stage, N stage, and age) had a higher risk score (**Fig 5A**). Besides, the risk score was higher in patients with low oxidative stress score those showing high oxidative stress score ($p = 1.1e\text{-}05$) (**Fig 5A**). High-risk patients had higher clinical grade and most low-risk patients had higher oxidative stress score (**Fig 5B**). Comparison on the prognosis difference between risk score types showed a high reliability among different clinicalpathological groups (**Fig 5C**).

Fig. 5. Association between the clinicopathological features and oxidative stress score and risk score of prostate cancer. **A** Differences in risk score between clinicopathological characteristics as well as oxidative stress score groups. **B** Distribution of 683 clinicopathological characteristics between high- and low-risk patients. The upper part is statistically significant -$\log_{10}$ (p value), the lower part is the proportion. **C** Kaplan-Meier curve for high- and low-risk patients with different clinicopathological characteristics in TCGA-PRAD cohort. P < 0.05 was considered statistically significant.

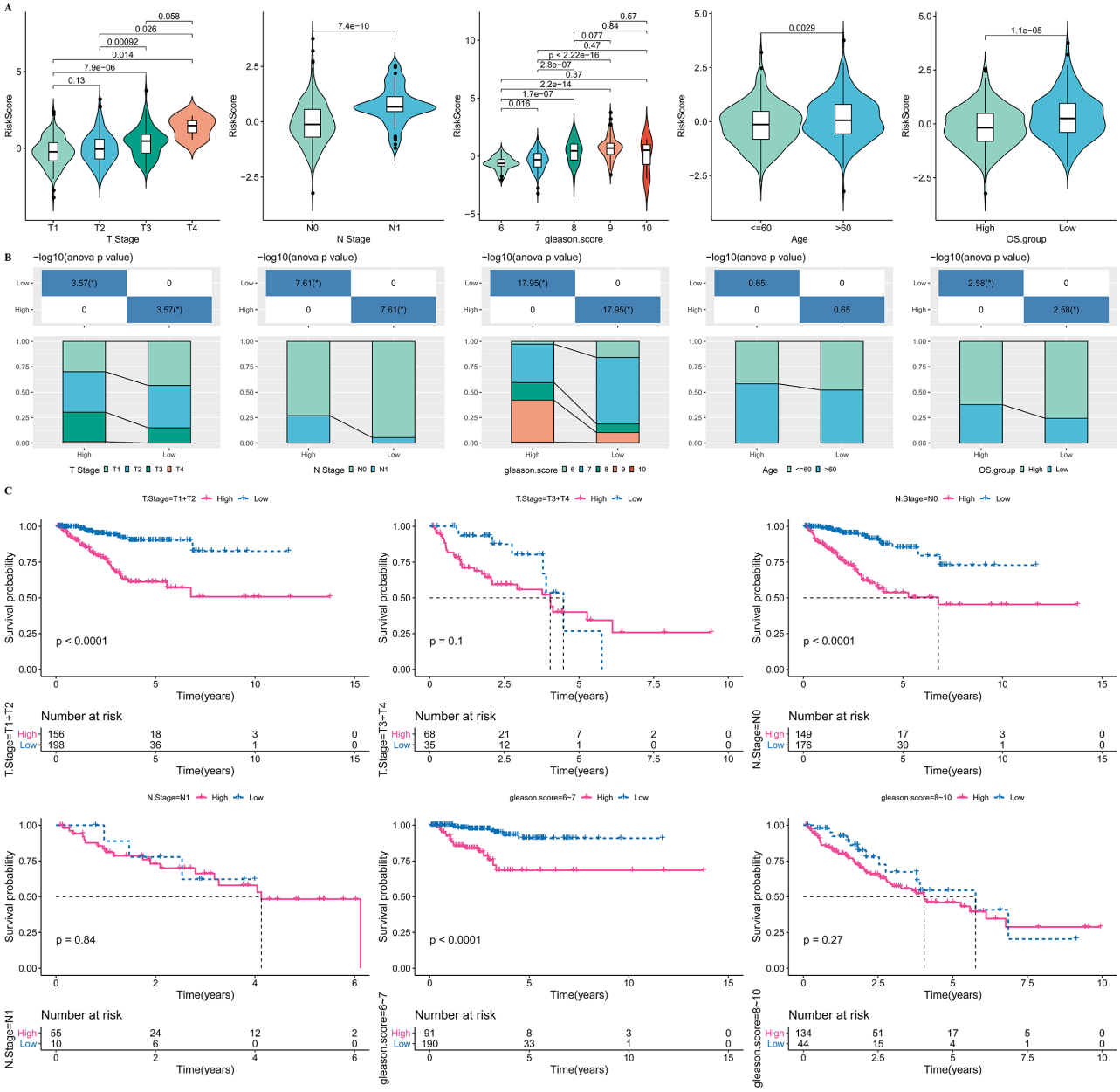

Fig. 6. Gene mutation characteristics analysis between high- and low-risk groups in TCGA-PRAD cohort. **A** Distributions of gene mutation-related features between the two risk types. **B** Correlation analysis between risk score and gene mutation-related features. **C** The top 20 mutated genes in the two risk groups. Statistically significant was defined when p < 0.05.

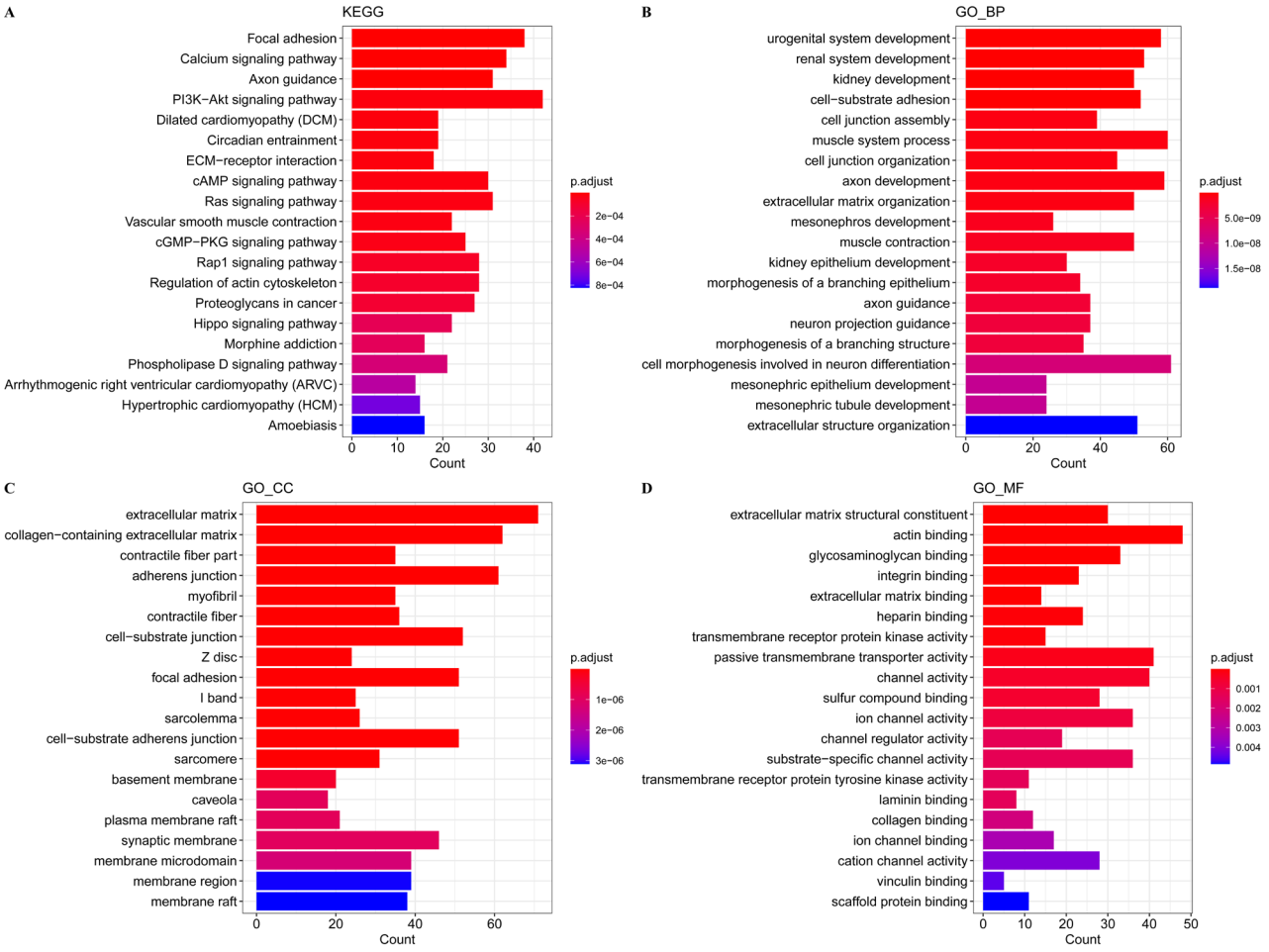

Enrichment analysis

Functional enrichment analysis in brown module was performed (**Supplementary Table 2**). 58 pathways (FDR < 0.05) were enriched through KEGG enrichment analysis, and **Fig 6A** displayed top20 pathways mainly including PI3K-Akt signaling pathway, Focal adhesion, Vascular smooth muscle contraction, ECM-receptor interaction, Calcium signaling pathway, which were correlated with the tumor initiation and progression. The three terms of the GO functional enrichment analysis were analyzed (**Fig 6B-D**). The top GO-BP enriched pathways were listed in **Fig 6B**. The genes in brown module were largely enriched in the cell matrix-related pathway.

The high-risk group had some enriched pathways related to cell cycle and cell matrix, including KEGG_SPLICEOSOME, KEGG_CELL_CYCLE, and KEGG_ECM_RECEPTOR_INTERACTION. Moreover, several immune-related pathways such as KEGG_ TOLL_ LIKE_ RECEPTOR_ SIGNALING_ PATHWAY, KEGG_ INTESTINAL_ IMMUNE_ NETWORK_ FOR_ IGA_ PRODUCTION, KEGG_ CYTOKINE_ CYTOKINE_ RECEPTOR_ INTERACTION, KEGG_ PRIMARY_ IMMUNODEFICIENCY, KEGG_ CHEMOKINE_ SIGNALING_ PATHWAY, KEGG_ NOD_ LIKE_ RECEPTOR_ SIGNALING_ PATHWAY were greatly enriched in patients showing a high risk (**Fig 7A**).

Meanwhile, GSEA analysis was performed with all candidate gene sets in Hallmark database [39] (**Fig 7B**). Furthermore, a total of 19 differentially expressed biological pathways among different risk types. Pathways related to cell cycle and metabolism were significantly enriched in high-risk and low-risk groups, respectively (**Fig 7C**). Risk score was remarkably negatively correlated with some metabolic pathways, such as XENOBIOTIC_METABOLISM, FATTY_ACID_METABOLISM, and BILE_ACID_ METABOLISM, while it had significant positive correlation with cell cycle-related pathways (**Fig 7D**).

Fig. 7. Pathway enrichment analyses between two risk types in TCGA-PRAD cohort. **A** GSEA analysis with all the KEGG gene sets in different risk types. **B** Heatmap of ssGSEA score. **C** Differential pathways between two risk types. **D** Correlation analysis was performed on the connections between differential pathways and the risk score. ***p <0.001, and ****p <0.0001.

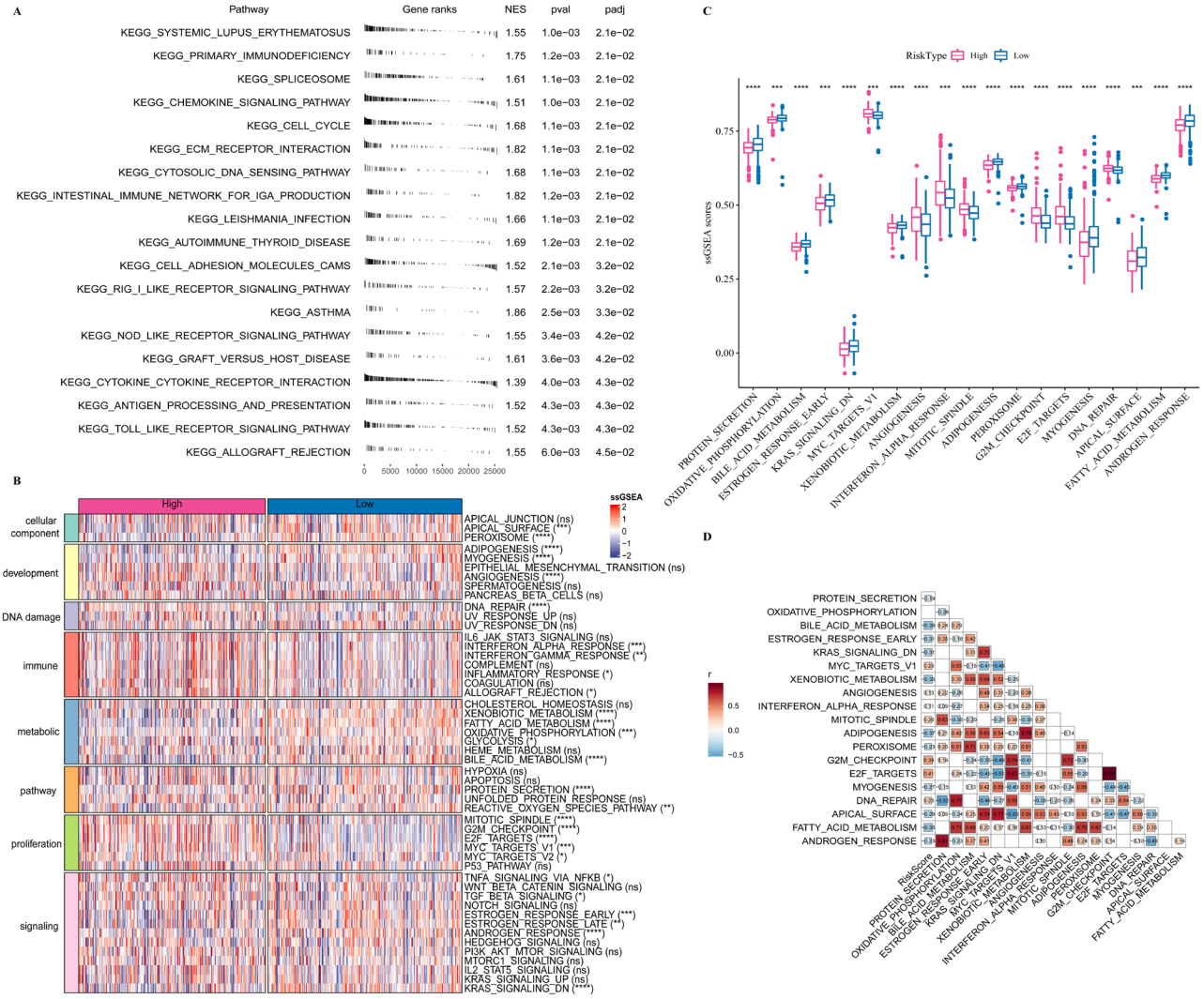

Fig. 8. Distinct TME characteristics of prostate cancer patients. **A** Differences in ESTIMATE scores in two risk types. **B** Boxplots of 22 infiltrating immune cell types. **C** Correlation analysis between 22 infiltrating immune cells and the risk score. **D** Distributions of 29 TME-related gene signatures. **E** PROGEN was used to measure the relative signaling pathway activity scores in the tumor cells, and the results were visualized into boxplots. *p < 0.05, **p <0.01, ***p <0.001, and ****p <0.0001.

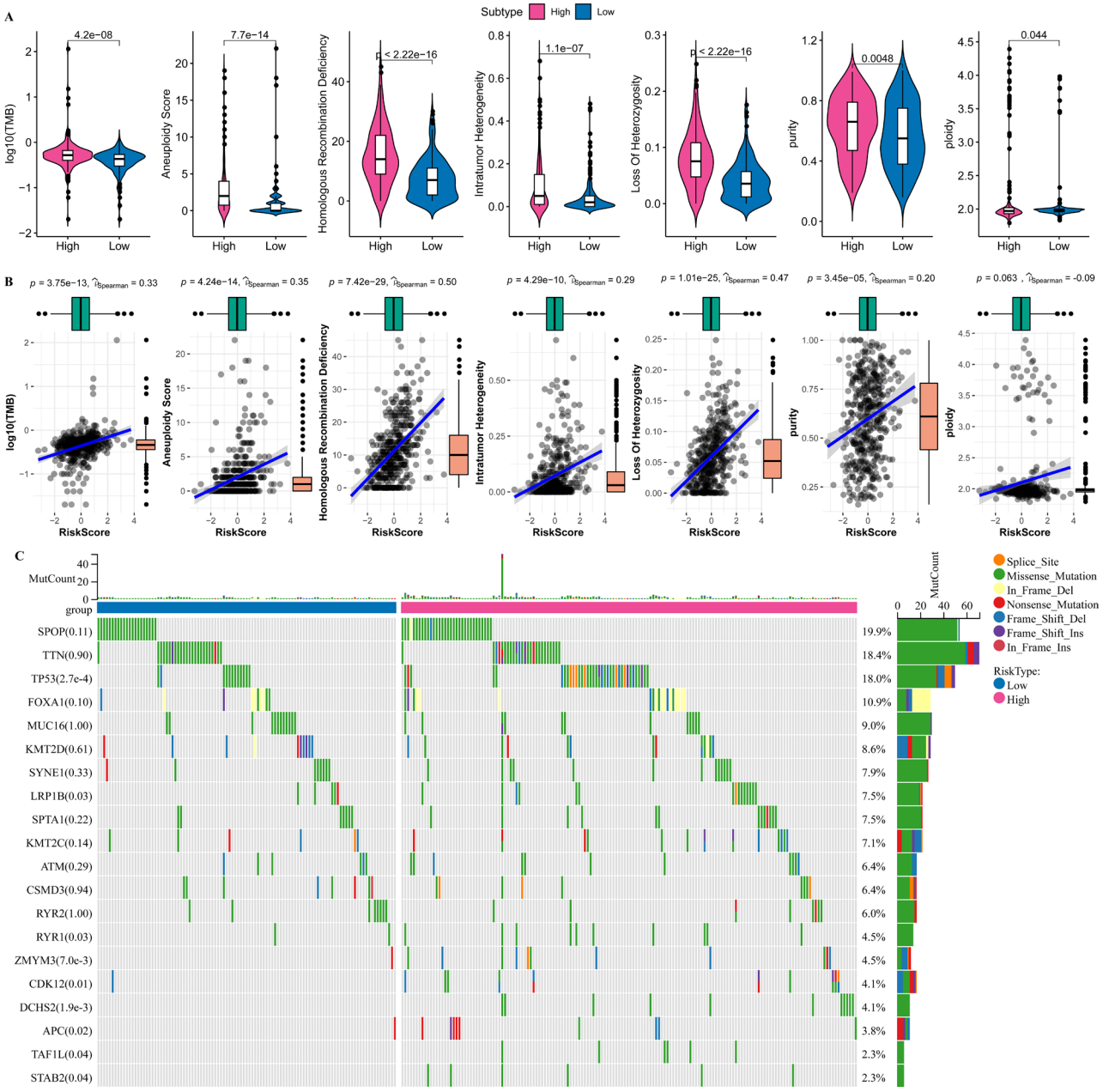

Gene mutation characteristics analysis in patients

Further, we explored the differences in genomic changes between the two risk groups in the TCGA cohort. It was observed that the high-risk group had higheraneuploidy score (p = 7.7e-14), tumor mutation burden (TMB) (p = 4.2e-08), homologous recombination defects (p < 2.22e-16), intratumor heterogeneity (p = 1.1e-07), loss of heterozygosity (p < 2.22e-16), and purity (p = 0.0048) (**Fig 8A**). **Fig 8B** depicted that risk score showed a significant positive correlation with TMB (p = 3.7e-13, ρs = 0.33), aneuploidy score (p = 4.24e-14, ρs = 0.35), homologous recombination defects (p = 7.42e-29, ρs = 0.50), intratumor heterogeneity (p = 4.29e-10, ρs = 0.29), loss of heterozygosity (p = 1.01e-25, ρs = 0.47), and purity (p = 3.45e-05, ρs = 0.20). Analysis on somatic mutation differences between high- and low- risk groups showed significantly different mutation frequencies of several genes such as SPOP, TTN, and TP53 between the two groups (**Fig 8C**).

Fig. 9. Sensitivity of prostate cancer patients with two risk types to antitumor therapy. **A** Difference in "T cell inflamed GEP score" between two risk types. **B** Difference in "Th1/IFNγ gene signature" between two risk types. **C** Difference in "Cytolytic activity" between two risk types. **D** Differential expression patterns of several immune checkpoint genes between two risk types. **E** Responsiveness to ICI therapy between two risk types. **F** The association between risk score types and drug responses in cancer cell lines. **G** The box plots of the estimated IC50 for Cisplatin, Bicalutamide, and Docetaxel in TCGA-PRAD. *p < 0.05, **p <0.01, ***p <0.001, and ****p <0.0001.

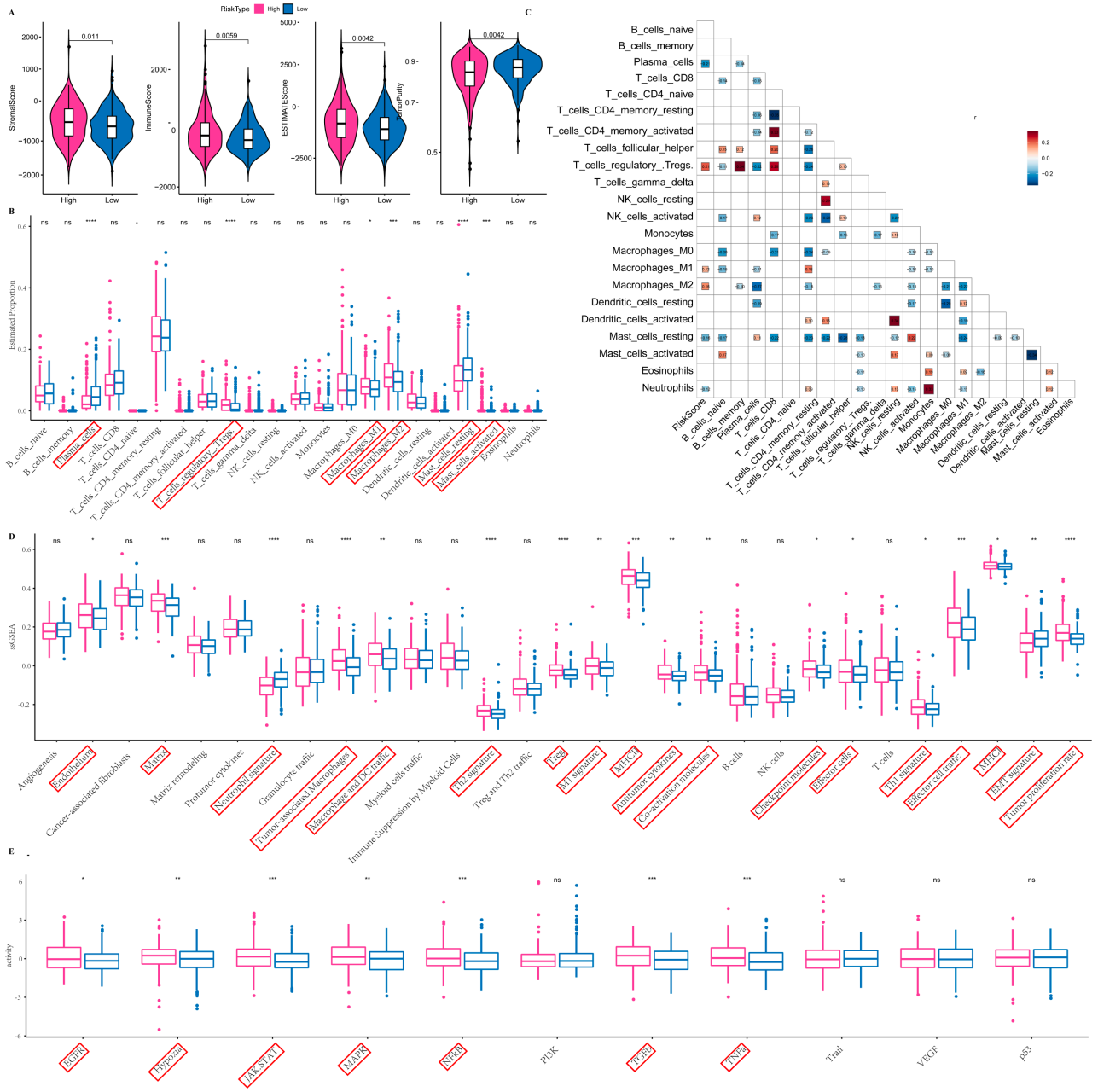

Different tumor microenvironment (TME) characteristics of patients

The results of ESTIMATE analysis demonstrated that high-risk patients had a lower TumorPurity but higher ESTIMATEScore, StromalScore, ImmuneScore (**Fig 9A**). Additionally, the CIBERSORT results showed that the Mast_ cells_ resting, Plasma_ cells, and T_ cells_ CD8 were remarkably enriched in low-risk patients, while high-risk patients had abundant T_ cells_ regulatory_ Tregs and Macrophages_ M2 (**Fig 9B**). **It** showed a significant positive correlation between Macrophages_ M2 and T_ cells_ regulatory_ Tregs and the risk score, whereas risk score and Plasma_cells were significantly negatively related. (**Fig 9C**)

The ssGSEA analysis demonstrated that high-risk patients had significantly enriched matrix components such as matrix and matrix remodeling and cancer-associated fibroblasts. In addition, high-risk patients had the highest tumor proliferation rate

Fig. 10. The prognosis of PRAD patients predicted a nomogram. **A-B** The prognostic significance of clinicopathological features and the risk score tested by univariate and multivariate Cox regression analysis. **C** The 1-, 3-, and 5-year OS of prostate cancer patients was evaluated with the nomogram. **D** Validation on the prediction by the nomogram reflected in calibration curves. **E-F** The 1-, 3-, and 5-year OS of prostate cancer patients predicted by the nomogram was tested by decision curve analysis. *p < 0.05, **p <0.01, 724 and ***p <0.001.

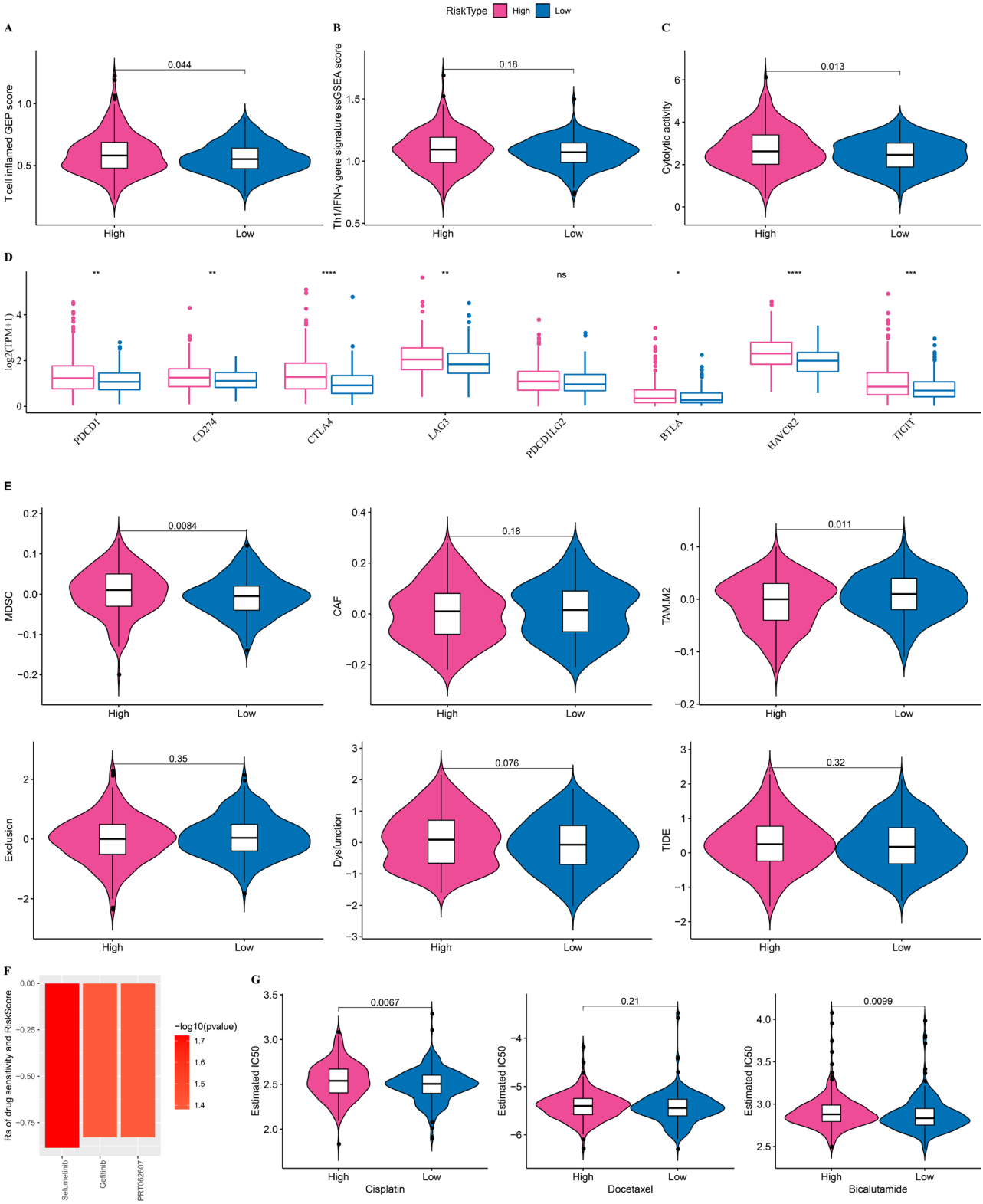

Fig. 11. The prognosis of PRAD patients predicted a nomogram. A-B, Prognostic significance of clinicopathological features and the risk score tested by univariate and multivariate Cox regression analysis. C, 1-, 3-, and 5-year OS of PRAD patients was evaluated with the nomogram. D, Validation on the prediction by the nomogram reflected in calibration curves. E-F, 1-, 3-, and 5-year OS of PRAD patients predicted by the nomogram was tested by DCA. $^{*}p < 0.05$, $^{**}p < 0.01$, and $^{***}p < 0.001$.

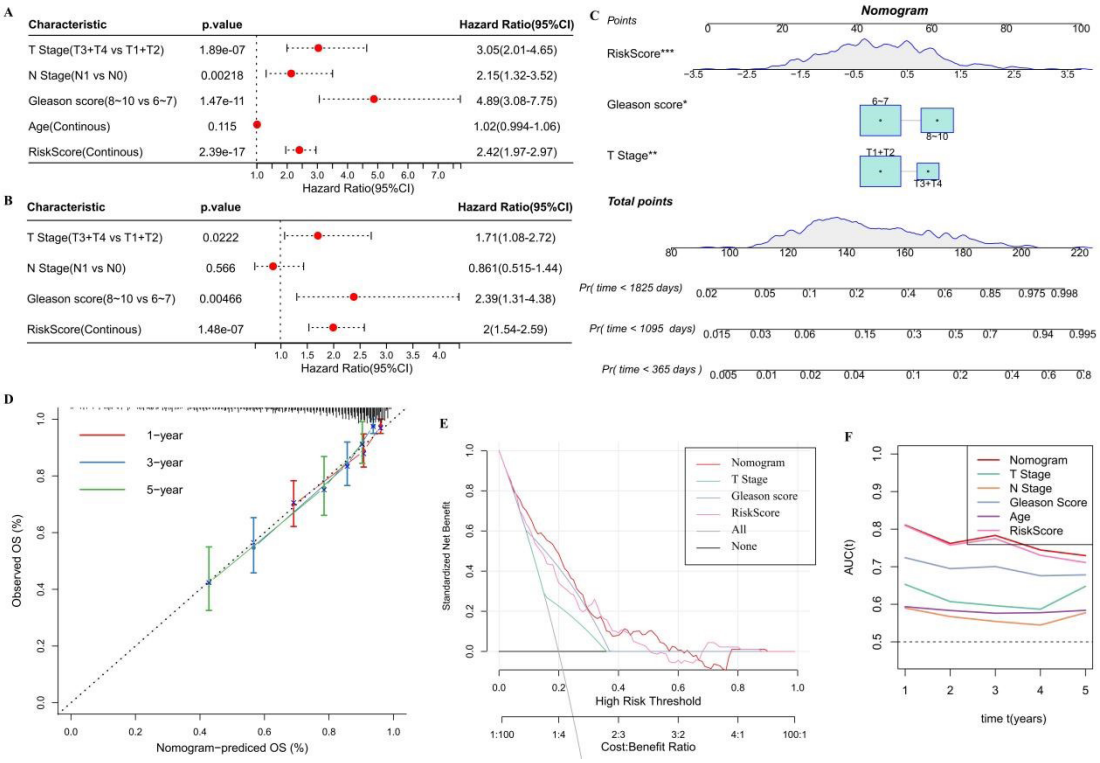

score (**Fig 9D**). Besides, various pathways including EGFR, hypoxia, JAK-STAT, MAPK, NF-κB, TGFb, and TNFα were activated in high-risk patients (**Fig 9E**).

Sensitivity prediction of patients to antitumor therapy with different risk scores

"T-cell-inflated GEP score" was used to test the potential response of patients with two risk types to immunotherapy. "T-cellinflated GEP score" in the high-risk group was significantly increased (**Fig 10A**). Considering IFN-γ is a cytokine that fulfills a key role in anti-cancer immunity and immune regulation, we obtained Th1/IFNγ gene signature from the previous study [40] and calculated the ssGSEA score for the Th1/IFNγ gene signature. It was found that low-risk patients had a higher Th1/IFNγ score (**Fig 10B**), while high-risk patients showed a higher cytolytic activity (CYT) score (**Fig 10C**). We evaluated some representative immune checkpoint genes and observed that high risk score group had significantly high-expressed key immune checkpoint genes, such as PDCD1, CD274, CTLA4, LAG3, PDCDILG2, BTLA, TIGIT, and HAVCR2 (**Fig 10D**).

No significant differences in TIDE score between the two risk types were observed but high-risk patients had a higher MDSC score (**Fig 10E**). Analysis on the association between risk score types and drug responses in cancer cell lines revealed three pairs in GDSC database showing that drug sensitivity was related to the risk score (**Fig 10F**). Low-risk patients in TCGA-PRAD had higher sensitivities to the traditional chemotherapy drugs (Bicalutamide, Cisplatin, and Docetaxel) (**Fig 10G**).

A nomogram for the prognostic prediction

Whether the risk score and several clinicopathological features were independent prognostic factors for prostate cancer patients was evaluated by performing univariate and multivariate Cox regression analyses, the results of which verified that the risk score was an independent factor for prostate cancer prognosis (**Fig 11A-B**). A nomogram integrating the clinicopathological features (T stage, N stage, gleason score, and age) and the risk score was built to estimate 1-, 3-, and 5-year OS, and the risk score showed the greatest impact on OS of prostate cancer patients (**Fig 11C**). The observed and predicted calibration curves of the nomogram was highly consistent (**Fig 11D**). Further DCA analysis also confirmed that both the risk score and the nomogram had the most powerful influence on the prognostic prediction for prostate cancer (**Fig 11E-F**).

Discussion

Redox homeostasis plays pivotal role in the maintenance of normal physiological functions. Oxidative stress is the excessive production of ROS resulting from the imbalance between antioxidants and oxidants in tumor cells, and increased oxidative stress promotes tumor growth, survival and progression [41]. Accumulating studies revealed that oxidative stress contribute to antitumor immune response, suggesting oxidative stress can be used as a new target for anticancer therapy [42]. Currently, we lacked a comprehensive analysis on the roles of oxidative stress-related gene signature in the prognostic prediction and its therapeutic importance in prostate cancer. Therefore, this study used the ssGSEA algorithm to compute oxidative stress score for TCGA-PRAD samples, and we found that higher ssGSEA score for oxidative stress predicted prolonged OS in prostate cancer patients. WGCNA classified 37 modules related to oxidative stress and 680 hub genes were screened from the key module, that is, the brown module. Afterwards, 6 hub genes (NUDT7, NTRK3, MAP3K12, DRD5, C3orf18, and B3GALT2) were identified after COX regression and LASSO analysis. Further risk model was developed using the 6 prognostic genes, with patients with a higher risk score having worse prognosis. Cox analysis confirmed the risk score as an independent factor for prostate cancer prognosis. The current nomogram together with calibration curves and DCA analysis all confirmed the powerful in predicting the prognosis.

This study established six oxidative stress-related gene signatures (NUDT7, NTRK3, MAP3K12, DRD5, C3orf18, and B3GALT2) as an independent factor for the prognostic survival of prostate cancer. NUDT7, a Nudix domain-containing protein, encodes a peroxisomal nudix hydrolase specific for coenzyme A and its derivatives. It has been reported that knockdown of NUDT7 in arabidopsis increases susceptibility to paraquat-induced oxidative stress [43]. In addition, NUDT7 serves as a potent tumor suppressor to inhibit the progression of $Kras^{G12D}$ colorectal cancer [44]. The elevated expression of fusion gene ETV6-NTRK3 triggers the expression of cystine/glutamate antiporter xCT and promotes oncogenic RAS transformation via preserving intracellular redox homeostasis [45]. AK005401/MAP3K12 pathway is crucial in oxidative stress-associated hippocampal injury, and application of celastrol can potentially attenuate the neuronal injury through inhibiting AK005401/MAP3K12 pathway [46]. A previous study has confirmed that activating DRD5 promotes the production of ROS, inhibits the MTOR pathway, and enhances macroautophagy/ autophagy, which results in cell death in tumor cells [47]. Dopamine aggravates esophageal cancer cell proliferation and growth through the DRD5-mediated pathway *in vitro* and *in vivo* [48]. C3orf18 is a differentially expressed gene associated with the anti-oxidative stress ability of rho kinase inhibitors on trabecular meshwork cells [49]. B3GALT2 belongs to β-1, 3-galactosyltransferase family, and has an inhibitory effect on ischemia/reperfusion-induced neuron apoptosis and oxidative stress [50]. The cellular experiments showed that knockdown MAP3K12 inhibited PCa cell viability. Collectively, these findings suggested that the prognostic genes in the current gene signature may be crucial in oxidative stress response during prostate cancer development and progression.

Gene mutation plays a prominent role in the initiation and development of malignant cancers [51]. The increased TMB status and mutated driver genes are highly associated with a higher risk of African prostate cancer [52]. Frequent mutation of TP53, PTEN, and RB1 can predict a poor prognosis not only at early stage but advanced stage for prostate cancer patients and guide prospective treatments [53]. It has been proven that mutated genes participate in the disrupted redox homeostasis for prostate cancer, and that SPOP was the most mutated in the low-risk patients, while TP53 was the driver gene with the greatest mutation in the high-risk patients [54]. Meanwhile, spontaneous single TTN mutation represents an elevated TMB [55]. This study found that the risk score was significantly correlated positively with TMB, and that the mutation frequency of several genes such as SPOP, TTN, and TP53 was significantly different between the two risk groups. Our findings indicated that the risk model can predict the gene mutation status for prostate cancer patients.

It is known that anti-cancer therapy such as radiotherapy affects the TME and better understanding the immune response may contribute to the optimization of therapy. Inflammatory cells including M2 macrophages and Tregs are reported to be implicated in cancer progression through suppressing the anti-tumor immune response [56]. A previous study has demonstrated that increased numbers of M2 macrophages in TME of the prostate cancer patients lead to increased mortality rate, and that M2 macrophages together with Tregs may promote an immunosuppressive environment [57].

On the contrast, the plasma cells are positively involved in antitumor immune response, and hormone receptor-negative breast cancer patients with increased numbers of plasma cells exhibit a favorable outcome, indicating that enhancement of plasma cell responses can be considered as a target for tumor therapy [58]. Our findings suggested that the risk score was positively correlated with T_cells_ regulatory_Tregs and Macrophages_M2 but negatively correlated with Plasma_cells. It has been shown that patients with various malignancies will benefit from ICI therapy. CTLA4, PDCD1 (PD-1), CD274 (PD-L1) are common targets for ICI therapy. Recently, novel potential molecules as well as their ligands are considered for ICB therapy, such as LAG3, BTLA, TIGIT, PDCDILG2, and HAVCR2 [59, 60]. In this study, we also evaluated some representative immune checkpoint genes, and found that PDCD1, TLA4, LAG3, CD274, CPDCDILG2, HAVCR2, TIGIT, and BTLA were high-expressed in high-risk patients. These findings showed that our oxidative stress-based risk model could serve as a specific predictive approach for immunotherapy in prostate cancer patients. Timely identification and intervention of key immunosuppressive promotors in the TME, such as MDSC, may be promising approaches to the improvement of ICI therapy [61]. In current study, the two risk types showed no significant difference in TIDE score, but high-risk patients had a higher MDSC score. Therefore, prostate cancer patients may benefit from the therapy targeting MDSC, and further studies are needed to confirm our results. Additionally, low-risk patients had higher sensitivity to conventional chemotherapy drugs, especially Bicalutamide and Cisplatin, suggesting that oxidative stress-based risk scores may accurately predict the anti-tumor immune responses and facilitate the development of individualized therapeutic strategy.

The present study had some limitations. Firstly, this study analyzed the data from public database TCGA as a training data set and GEO database as a validation data, and these retrospective data were restricted by selection bias that could affect the reliability of our results. Thus, prospective studies with more samples are encouraged to further verify our retrospective results. Secondly, except for the data on gleason score, age, T Stage, N Stage in the public database, more clinicopathological characteristics should be included. Thirdly, the accuracy of our risk model has been verified in this study, but its applicability for long-term clinical use should be tested.

Conclusion

To conclude, the integrated bioinformatics analysis identified 6 genes related to oxidative stress for prostate cancer patients. The oxidative stress gene signature was significantly related to OS, clinicopathological characteristics, and the TME of prostate cancer patients. The risk model also showed an accurate prediction for therapeutic responses. The current findings validated the clinical importance of the oxidative stress score in the prognosis prediction and personalized anti-tumor therapies.

Declarations

Funding

This study was supported by grants from the National Natural Science Foundation of China (82203428).

Competing interests

The author(s) declare no conflict of interest.

Author contributions

All authors contributed to this present work: [BHX] and [SL] designed the study, [KY] acquired the data. [KY] and [BHX] improved the figure quality. [SL] and [KY] drafted the manuscript, [BHX] and [SL] revised the manuscript. All authors read and approved the manuscript.

Data availability

The datasets generated and/or analyzed during the current study are available in the [GSE70769] repository, [https://www.ncbi.nlm.nih.gov/geo/query/acc.cgi?acc= GSE70769].

Ethical approval and consent to participate

Not applicable

Consent for publication

Not applicable

Acknowledgements

Not applicable

Abbreviations

PRAD, prostate adenocarcinoma
TCGA, The Cancer Genome Atlas
GEO, Gene-Expression Omnibus
MsigDB, Molecular Signatures Database
WGCNA, the weighted gene coexpression network
ICI, immune checkpoint inhibition

TIDE, tumor immune dysfunction exclusion
GDSC, Genomics of Drug Sensitivity in Cancer
ssGSEA, single-sample gene set enrichment analysis
OS, overall survival
stepAIC, stepwise Akaike information criterion
ROC, receiver operating characteristic analysis
AUC, area under ROC curve
LASSO, least absolute shrinkage and selection operator
ICB, immune checkpoint blockade
CAF, M2 subtype of tumor-associated fibroblasts
MDSCs, myeloid-derived suppressor cells
TAM, tumor-associated macrophages
CTLs, cytotoxic T lymphocytes
CYT, cytolytic activity
DCA, Decision curve analysis
FDR, false discovery rate
IFN-γ, interferon-gamma
TME, tumor microenvironment
TMB, tumor mutation burden
BP, Biological process
CC, Cellular component
MF, Molecular function

References

1. Inamura K: **Prostatic cancers: Understanding their molecular pathology and the 2016 WHO classification**. *Oncotarget* 2018, **9**(18):14723.
2. Sung H, Ferlay J, Siegel RL, Laversanne M, Soerjomataram I, Jemal A, Bray F: **Global cancer statistics 2020: GLOBOCAN estimates of incidence and mortality worldwide for 36 cancers in 185 countries**. *CA: a cancer journal for clinicians* 2021, **71**(3):209-249.
3. Aragon-Ching JB, Dahut WL: **VEGF inhibitors and prostate cancer therapy**. *Current molecular pharmacology* 2009, **2**(2):161-168. doi: 10.2174/1874467210902020161. PMC2711630.
4. Ebrahimi S, Hashemy SI, Sahebkar A, Aghaee Bakhtiari SH: **MicroRNA Regulation of Androgen Receptor in Castration-Resistant Prostate Cancer: Premises, Promises, and Potentials**. *Current molecular pharmacology* 2021, **14**(4):559-569. doi: 10.2174/1874467213666201223121850.
5. Duan H, Xu B, Xie T: **The preventive mechanisms and research progress of sulforaphane in relation to prostate cancer**. *Biocell* 2024, **0**(0):1-10. doi: 10.32604/biocell.2024.054873.
6. Bray F, Laversanne M, Sung H, Ferlay J, Siegel RL, Soerjomataram I, Jemal A: **Global cancer statistics 2022: GLOBOCAN estimates of incidence and mortality worldwide for 36 cancers in 185 countries**. *CA Cancer J Clinicians* 2024, **74**(3):229-263. doi: https://doi.org/10.3322/caac.21834.
7. Duffy MJ: **Biomarkers for prostate cancer: prostate-specific antigen and beyond**. *Clinical Chemistry and Laboratory Medicine (CCLM)* 2020, **58**(3):326-339.
8. Hansen A, Massard C, Ott P, Haas N, Lopez J, Ejadi S, Wallmark J, Keam B, Delord J-P, Aggarwal R: **Pembrolizumab for advanced prostate adenocarcinoma: findings of the KEYNOTE-028 study**. *Annals of Oncology* 2018, **29**(8):1807-1813.
9. Cha H-R, Lee JH, Ponnazhagan S: **Revisiting Immunotherapy: A Focus on Prostate CancerAdvances and Limitations of Immunotherapy in Prostate Cancer**. *Cancer research* 2020, **80**(8):1615-1623.
10. Denham JW, Joseph D, Lamb DS, Spry NA, Duchesne G, Matthews J, Atkinson C, Tai K-H, Christie D, Kenny L: **Short-term androgen suppression and radiotherapy versus intermediate-term androgen suppression and radiotherapy, with or without zoledronic acid, in men with locally advanced prostate cancer (TROG 03.04 RADAR): 10-year results from a randomised, phase 3, factorial trial**. *The Lancet Oncology* 2019, **20**(2):267-281.
11. Chen K, Lu P, Beeraka NM, Sukocheva OA, Madhunapantula SV, Liu J, Sinelnikov MY, Nikolenko VN, Bulygin KV, Mikhaleva LM: **Mitochondrial mutations and mitoepigenetics: Focus on regulation of oxidative stress-induced responses in breast cancers**. In: *Seminars in Cancer Biology: 2020*: Elsevier; 2020.
12. Fu Y, Chung F-L: **Oxidative stress and hepatocarcinogenesis**. *Hepatoma research* 2018, **4**.
13. Ahmed AM: **The dual role of oxidative stress in lung cancer**. In: *Oxidative Stress in Lung Diseases.* edn.: Springer; 2019: 99-113.
14. Peng D, Lu H, Zhu S, Zhou Z, Hu T, Chen Z, Zaika A, El-Rifai W: **NRF2 antioxidant response protects against acidic bile salts-induced oxidative stress and DNA damage in esophageal cells**. *Cancer letters* 2019, **458**:46-55.
15. Sies H, Berndt C, Jones DP: **Oxidative stress**. *Annual review of biochemistry* 2017, **86**:715-748.
16. Hayes JD, Dinkova-Kostova AT, Tew KD: **Oxidative stress in cancer**. *Cancer cell* 2020, **38**(2):167-197.

17. Sönmez MG, Kozanhan B, Deniz ÇdD, Göger YE, Kılınç MT, Neşeliogˇlu S, Erel Ö: **Is oxidative stress measured by thiol/disulphide homeostasis status associated with prostate adenocarcinoma?** *Central European Journal of Immunology* 2018, **43**(2):174-179.
18. Liguori I, Russo G, Curcio F, Bulli G, Aran L, Della-Morte D, Gargiulo G, Testa G, Cacciatore F, Bonaduce D: **Oxidative stress, aging, and diseases**. *Clinical interventions in aging* 2018, **13**:757.
19. Wilson TK, Zishiri OT: **Prostate Cancer: A Review of Genetics, Current Biomarkers and Personalised Treatments**. *Cancer Reports* 2024, **7**(10):e70016. doi: https://doi.org/10.1002/cnr2.70016.
20. Chen X, Jin Y, Gong L, He D, Cheng Y, Xiao M, Zhu Y, Wang Z, Cao K: **Bioinformatics analysis finds immune gene markers related to the prognosis of bladder cancer**. *Frontiers in Genetics* 2020, **11**:607.
21. Hu D, Cao Q, Tong M, Ji C, Li Z, Huang W, Jin Y, Tong G, Wang Y, Li P: **A novel defined risk signature based on pyroptosis-related genes can predict the prognosis of prostate cancer**. *BMC medical genomics* 2022, **15**(1):1-17.
22. Ritchie ME, Phipson B, Wu D, Hu Y, Law CW, Shi W, Smyth GK: **limma powers differential expression analyses for RNA-sequencing and microarray studies**. *Nucleic acids research* 2015, **43**(7):e47-e47.
23. Langfelder P, Horvath S: **WGCNA: an R package for weighted correlation network analysis**. *BMC bioinformatics* 2008, **9**(1):1-13.
24. Hastie T, Qian J, Tay K: **An Introduction to glmnet**. *CRAN R Repositary* 2021.
25. Blanche P: **TimeROC: Time-dependent ROC curve and AUC for censored survival data**. *R package version* 2015, **2**.
26. Hänzelmann S, Castelo R, Guinney J: **GSVA: gene set variation analysis for microarray and RNA-seq data**. *BMC bioinformatics* 2013, **14**(1):1-15.
27. Kassambara A, Kosinski M, Biecek P, Fabian S: **survminer: Drawing Survival Curves using 'ggplot2'**. *R package version 03* 2017, **1**.
28. Korotkevich G, Sukhov V, Budin N, Shpak B, Artyomov MN, Sergushichev A: **Fast gene set enrichment analysis**. *BioRxiv* 2021:060012.
29. Yu G, Wang L-G, Han Y, He Q-Y: **clusterProfiler: an R package for comparing biological themes among gene clusters**. *Omics: a journal of integrative biology* 2012, **16**(5):284-287.
30. Kassambara A: **ggcorrplot: Visualization of a Correlation Matrix using'ggplot2'**. *R package version 01* 2019, **3**.
31. V T, DL G, SD B, D W, DS B, TH OY, E P-P, GF G, CL P, JA E *et al*: **The Immune Landscape of Cancer**. *Immunity* 2018, **48**(4):812-830.e814. doi: 10.1016/j.immuni.2018.03.023.
32. Chen B, Khodadoust MS, Liu CL, Newman AM, Alizadeh AA: **Profiling tumor infiltrating immune cells with CIBERSORT**. In: *Cancer systems biology*. edn.: Springer; 2018: 243-259.
33. Yoshihara K, Shahmoradgoli M, Martínez E, Vegesna R, Kim H, Torres-Garcia W, Treviño V, Shen H, Laird PW, Levine DA: **Inferring tumour purity and stromal and immune cell admixture from expression data**. *Nature communications* 2013, **4**(1):1-11.
34. Bagaev A, Kotlov N, Nomie K, Svekolkin V, Gafurov A, Isaeva O, Osokin N, Kozlov I, Frenkel F, Gancharova O: **Conserved pan-cancer microenvironment subtypes predict response to immunotherapy**. *Cancer cell* 2021, **39**(6):845-865. e847.
35. Schubert M, Klinger B, Klünemann M, Sieber A, Uhlitz F, Sauer S, Garnett MJ, Blüthgen N, Saez-Rodriguez J: **Perturbation-response genes reveal signaling footprints in cancer gene expression**. *Nature communications* 2018, **9**(1):1-11.
36. Jiang P, Gu S, Pan D, Fu J, Sahu A, Hu X, Li Z, Traugh N, Bu X, Li B: **Signatures of T cell dysfunction and exclusion predict cancer immunotherapy response**. *Nature medicine* 2018, **24**(10):1550-1558.
37. Geeleher P, Cox N, Huang RS: **pRRophetic: an R package for prediction of clinical chemotherapeutic response from tumor gene expression levels**. *PloS one* 2014, **9**(9):e107468.
38. Zhang Z, Kattan MW: **Drawing Nomograms with R: applications to categorical outcome and survival data**. *Annals of translational medicine* 2017, **5**(10):211. doi: 10.21037/atm.2017.04.01.
39. Liberzon A, Birger C, Thorvaldsdóttir H, Ghandi M, Mesirov JP, Tamayo P: **The molecular signatures database hallmark gene set collection**. *Cell systems* 2015, **1**(6):417-425.
40. Danilova L, Ho WJ, Zhu Q, Vithayathil T, De Jesus-Acosta A, Azad NS, Laheru DA, Fertig EJ, Anders R, Jaffee EM: **Programmed cell death ligand-1 (PD-L1) and CD8 expression profiling identify an immunologic subtype of pancreatic ductal adenocarcinomas with favorable survival**. *Cancer immunology research* 2019, **7**(6):886-895.

41. Chun K-S, Kim D-H, Surh Y-J: **Role of reductive versus oxidative stress in tumor progression and anticancer drug resistance**. *Cells* 2021, **10**(4):758.
42. Van Loenhout J, Peeters M, Bogaerts A, Smits E, Deben C: **Oxidative stress-inducing anticancer therapies: Taking a closer look at their immunomodulating effects**. *Antioxidants* 2020, **9**(12):1188.
43. Ge X, Li G-J, Wang S-B, Zhu H, Zhu T, Wang X, Xia Y: **AtNUDT7, a negative regulator of basal immunity in Arabidopsis, modulates two distinct defense response pathways and is involved in maintaining redox homeostasis**. *Plant physiology* 2007, **145**(1):204-215.
44. Song J, Park S, Oh J, Kim D, Ryu JH, Park WC, Baek I-J, Cheng X, Lu X, Jin E-J: **NUDT7 loss promotes KrasG12D CRC development**. *Cancers* 2020, **12**(3):576.
45. Lim JK, Delaidelli A, Minaker SW, Zhang H-F, Colovic M, Yang H, Negri GL, von Karstedt S, Lockwood WW, Schaffer P: **Cystine/glutamate antiporter xCT (SLC7A11) facilitates oncogenic RAS transformation by preserving intracellular redox balance**. *Proceedings of the National Academy of Sciences* 2019, **116**(19):9433-9442.
46. Wang C, Wan H, Li M, Zhang C: **Celastrol attenuates ischemia/reperfusion-mediated memory dysfunction by downregulating AK005401/MAP3K12**. *Phytomedicine* 2021, **82**:153441.
47. Leng ZG, Lin SJ, Wu ZR, Guo YH, Cai L, Shang HB, Tang H, Xue YJ, Lou MQ, Zhao W: **Activation of DRD5 (dopamine receptor D5) inhibits tumor growth by autophagic cell death**. *Autophagy* 2017, **13**(8):1404-1419.
48. Qian X, Zhang D, Cao Z, Ma H: **Dopamine pathway mediated by DRD5 facilitates tumor growth via enhancing Warburg effect in esophageal cancer**. *Frontiers in Oncology* 2021, **11**:655861.
49. Fujimoto T, Inoue T, Ohira S, Awai-Kasaoka N, Kameda T, Inoue-Mochita M, Tanihara H: **Inhibition of Rho kinase induces antioxidative molecules and suppresses reactive oxidative species in trabecular meshwork cells**. *Journal of Ophthalmology* 2017, **2017**:7598140. doi: 10.1155/2017/7598140.
50. Guo X, Zhang Y, Liu C, Ren L, Gao S, Bi J, Liang J, Wang P: **Intranasal administration of β-1, 3-galactosyltransferase 2 confers neuroprotection against ischemic stroke by likely inhibiting oxidative stress and NLRP3 inflammasome activation**. *The FASEB Journal* 2022, **36**(10):e22542.
51. Wijewardhane N, Dressler L, Ciccarelli FD: **Normal somatic mutations in cancer transformation**. *Cancer Cell* 2021, **39**(2):125-129.
52. Jaratlerdsiri W, Chan EK, Gong T, Petersen DC, Kalsbeek AM, Venter PA, Stricker PD, Bornman MR, Hayes VM: **Whole-genome sequencing reveals elevated tumor mutational burden and initiating driver mutations in African men with treatment-naïve, high-risk prostate cancer**. *Cancer research* 2018, **78**(24):6736-6746.
53. Hamid A, Gray K, Shaw G, MacConaill L, Evan C, Bernard B, Loda M, Corcoran N, Van Allen E, Choudhury A *et al*: **Compound Genomic Alterations of TP53, PTEN, and RB1 Tumor Suppressors in Localized and Metastatic Prostate Cancer**. *European urology* 2019, **76**(1):89-97. doi: 10.1016/j.eururo.2018.11.045.
54. Wu Y, Zhang X, Feng H, Hu B, Deng Z, Wang C, Liu B, Luan Y, Ruan Y, Liu X *et al*: **Exploration of Redox-Related Molecular Patterns and the Redox Score for Prostate Cancer**. *Oxidative medicine and cellular longevity* 2021, **2021**:4548594. doi: 10.1155/2021/4548594.
55. Oh J-H, Jang SJ, Kim J, Sohn I, Lee J-Y, Cho EJ, Chun S-M, Sung CO: **Spontaneous mutations in the single TTN gene represent high tumor mutation burden**. *NPJ genomic medicine* 2020, **5**(1):1-11.
56. Jarosz-Biej M, Smolarczyk R, Cichoń T, Kułach N: **Tumor microenvironment as a "game changer" in cancer radiotherapy**. *International journal of molecular sciences* 2019, **20**(13):3212.
57. Erlandsson A, Carlsson J, Lundholm M, Fält A, Andersson SO, Andrén O, Davidsson S: **M2 macrophages and regulatory T cells in lethal prostate cancer**. *The Prostate* 2019, **79**(4):363-369.
58. Sakaguchi A, Horimoto Y, Onagi H, Ikarashi D, Nakayama T, Nakatsura T, Shimizu H, Kojima K, Yao T, Matsumoto T: **Plasma cell infiltration and treatment effect in breast cancer patients treated with neoadjuvant chemotherapy**. *Breast Cancer Research* 2021, **23**(1):1-11.

59. Wagner M, Jasek M, Karabon L: **Immune Checkpoint Molecules—Inherited Variations as Markers for Cancer Risk**. *Frontiers in immunology* 2021, **11**:606721.
60. Tong Y, Yu Y, Zheng H, Wang Y, Xie S, Chen C, Lu R, Guo L: **Differentially Expressed Genes in Clear Cell Renal Cell Carcinoma as a Potential Marker for Prognostic and Immune Signatures**. *Frontiers in oncology* 2021, **11**:776824. doi: 10.3389/fonc.2021.776824. eCollection 2021.
61. Li T, Liu T, Zhu W, Xie S, Zhao Z, Feng B, Guo H, Yang R: **Targeting MDSC for Immune-Checkpoint Blockade in Cancer Immunotherapy: Current Progress and New Prospects**. *Clinical Medicine Insights: Oncology* 2021, **15**:11795549211035540.